NANO LETTERS

2007
Vol. 7, No. 2
318−322

Radiation Damping in Metal Nanoparticle Pairs

Christian Dahmen, Benjamin Schmidt,† and Gero von Plessen*

Institute of Physics (IA), RWTH Aachen University, D-52056 Aachen, Germany

Received October 10, 2006; Revised Manuscript Received December 17, 2006

ABSTRACT

The radiation damping rate of plasmon resonances in pairs of spherical gold nanoparticles is calculated. The radiative line width of the plasmon resonance indicates significant far-field coupling between the nanoparticles over distances many times the particle diameter. The radiation damping of the coupled particle−plasmon mode alternates between superradiant and subradiant behavior when the particle spacing is varied. At small particle spacings where near-field coupling occurs, the radiation damping rate lies far below that of an isolated particle.

Light impinging on a metal nanoparticle can resonantly excite a collective oscillation of the valence electrons known as particle plasmon.[1,2] When two or more nanoparticles are in close vicinity to each other, the localized particle plasmons of the individual nanoparticles interact via their optical near fields, forming coupled oscillation modes.[1,3−15] These coupled plasmon modes show large spectral shifts with respect to the localized particle plasmons of the individual nanoparticles[1,3,5,8,14,16−18] and huge enhancements of the local optical fields in the gaps between the particles.[4,6,7,9−11,13,19] The local-field enhancement has found much interest due to its use in nonlinear nanooptics applications such as surface-enhanced Raman spectroscopy.[4,20] Another effect of great interest is the occurrence of magnetic resonances in coupled pairs of specially shaped nanoparticles, which are expected to give rise to negative light refraction for use in optical metamaterials.[21,22]

One of the main impediments to the application of coupled plasmon modes are damping processes.[1,2,20,23,24] They shorten the coherent lifetime of the oscillation, broaden the plasmon resonance, and limit the local-field enhancement.[25] In principle, both nonradiative and radiative damping processes are present. Nonradiative processes such as electron scattering in the metal dissipate oscillation energy into heat and have been studied in great detail.[1,25−29] Radiative damping processes are caused by energy radiated into the optical far field by the collective electron oscillation and have been studied on single nanoparticles.[23,25,29−32] For instance, it has been shown that the radiative damping rate increases with particle size; this leads to a large broadening of the plasmon line at the largest nanoparticle sizes studied.[10,23,30,33] In contrast, little is known about radiation damping in coupled nanoparticles. A first indication that interesting effects may be expected from studies of radiation damping in such systems has been given by recent investigations of regular arrays of nanoparticles, where the line width was found to strongly depend on the particle spacing due to collective coupling of the particle plasmons to the far field.[14,34]

Here we present a theoretical study of radiation damping in pairs of metal nanoparticles, which may serve as a model system for more complex nanoparticle systems. We calculate the radiation damping rates of plasmon resonances in pairs of spherical gold nanoparticles using generalized Mie theory. We find that the radiative line width of the plasmon resonance indicates significant far-field coupling between the nanoparticles over distances many times the particle diameter. The radiation damping of the coupled particle−plasmon mode alternates between superradiant and subradiant behavior when the particle spacing is varied. At small particle spacings where near-field coupling occurs, the radiation damping rate lies far below that of an isolated particle. This reduction of radiation damping implies a reduced dephasing of the coupled plasmon mode and thus tends to increase the local field enhancement in the space between the particles.

Generalized Mie theory in the formulation of Gérardy and Ausloos[17,35,36] is employed to calculate light-scattering spectra of pairs of spherical gold nanoparticles, taking retardation effects into full account. We study the situation of two identical gold nanospheres of diameter $d = 80$ nm embedded in a transparent medium with an index of refraction $n = 1.51$. This choice of the embedding medium corresponds to the situation of particles on a glass substrate covered with index-matching liquid, a situation often encountered in microscopy experiments on metal nanoparticles.[25] The incident plane wave as well as the waves scattered by the particles are expanded in vector spherical harmonics in coordinate systems originating in the particles centers. In this

* Corresponding author. E-mail: gero.vonplessen@physik.rwth-aachen.de.
† Present address: Forschungszentrum Karlsruhe, Institut für Nanotechnologie, 76021 Karlsruhe, Germany and Institut für Theoretische Festkörperphysik, Universität Karlsruhe, 76128 Karlsruhe, Germany.

10.1021/nl062377u CCC: $37.00
Published on Web 01/23/2007

approach, no discretization of the surfaces of the particles takes place; instead, the boundary conditions imposed on the electromagnetic fields at the spherical surfaces are expressed in an infinite set of linear equations. This set of equations is truncated at a certain maximum multipole order to be numerically tractable. Depending on particle size and interparticle distance, the number of multipoles necessary for achieving convergence of the light-scattering spectra varies strongly.[17] For the smallest interparticle distance examined here (0.5 nm surface-to-surface distance, corresponding to a center-to-center distance of $D = 80.5$ nm), multipoles of maximum order 37 were included. With increasing interparticle distance, the contributions of higher-order multipoles to the light-scattering spectra diminish rapidly; for center-to-center distances D beyond ≈200 nm, calculations including only dipolar contributions give accurate results for the plasmon energies and linewidths of the nanoparticle pair examined here. A standard bulk dielectric function for gold was used in all calculations.[37] For center-to-center distances below 82 nm, we include a nonlocal dielectric response of the particles, following the approach described in refs 17 and 35.

The lower inset of Figure 1a shows a light-scattering spectrum of a pair of 80 nm gold nanoparticles with center-to-center distance $D = 290$ nm calculated by generalized Mie theory. The peak position of the particle−plasmon peak E_p (termed *plasmon energy* in the following) and the line width Γ are extracted from the light-scattering spectrum, as indicated in the inset. To study the particle plasmon resonance of gold nanoparticle pairs systematically, we plot Γ and E_p as a function of the interparticle distance D (Figure 1). Figure 1a is for polarization of the incident light wave perpendicular to the particle pair axis (transverse polarization), Figure 1b is for light polarization along the particle pair axis (longitudinal polarization, see insets). For both polarization directions, modulations of the plasmon energy and the line width as a function of the interparticle distance are seen. The plasmon energy and line width oscillate about their respective values for an isolated 80 nm sphere as obtained by Mie theory (indicated by horizontal lines). The initial modulation depth of the line width oscillations is as much as 30% of the line width calculated for the isolated particle. The decay length of the oscillations is different for the two polarization directions; for transverse polarization, the modulations are still observable at $D \approx 2$ μm, whereas for longitudinal polarization, the decay length is in the submicron range. The long-range oscillations of the line width and plasmon energy indicate that there is significant coupling between the particles over distances many times the particle diameter and thus far beyond the range of near-field coupling. The close agreement between the period of the oscillations and the wavelength corresponding to the plasmon energy (approximately 387 nm in a medium with $n = 1.51$)[38] suggests that this long-range coupling is mediated by the electromagnetic fields scattered by the particles. In the following, we wish to show that this is indeed the case.

Oscillations of the emission rate very similar to those of the line width observed here have been found in the emission

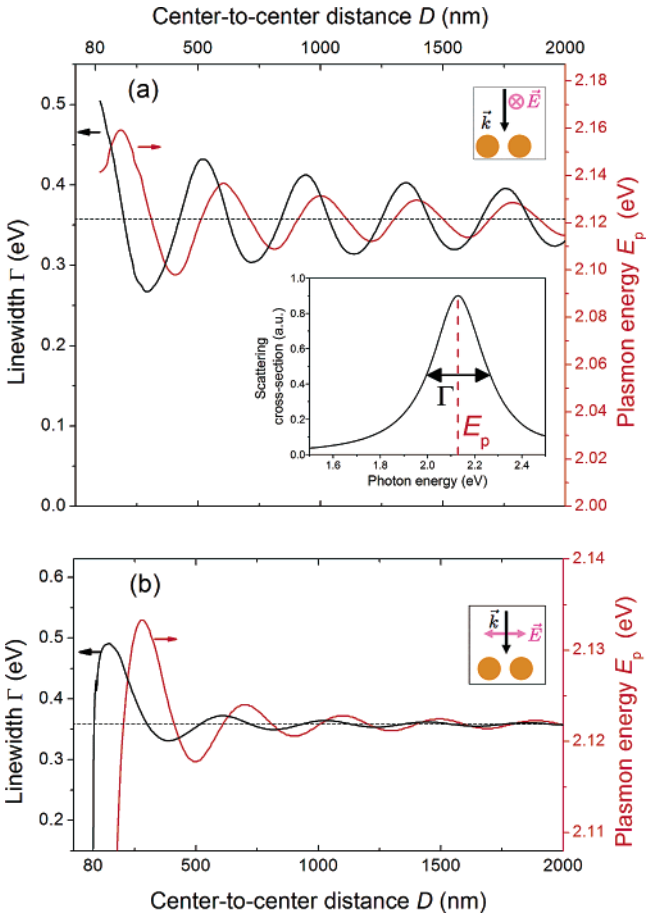

Figure 1. Calculated plasmon linewidths (fwhm, left axis) and plasmon energies (right axis) of a pair of 80 nm-gold nanospheres as functions of the center-to-center interparticle distance D. Every datapoint is extracted from a light-scattering spectrum (central inset: light-scattering spectrum calculated for $D = 290$ nm, transverse polarization). Figure 1a is for transverse polarization of the incident wave and Figure 1b is for longitudinal polarization (see insets). In both subfigures, the horizontal dashed lines indicate the plasmon line width and plasmon energy of an isolated 80 nm gold sphere.

from pairs of ions.[39,40] In this system, the spontaneous emission decay rate alternates between values higher and lower than that of an isolated ion when the distance between the ions is varied. In a classical picture, these alternations between superradiant and subradiant emission can be understood as resulting from the interference of the fields emitted by two classical dipoles. Emission is enhanced at those interion distances for which the fields from the two dipoles interfere constructively along the directions of highest emission intensity, i.e., perpendicular to the dipole axis. Conversely, emission is reduced at those interion distances for which interference along this direction is destructive. In the following, we will argue that the same interference principle is at the basis of the line width oscillations in Figure 1. For this purpose, we will compare our line width oscillations with those obtained from a calculation for the classical dipole pair used in ref 40. According to ref 40, the emission rate of two identical point dipoles spaced a distance D apart is, for transverse polarization and to leading order, given by $\gamma(D) = \gamma_0 \cdot (1 + 3\sin(2\pi D/\lambda)/(4\pi D/\lambda))$, where γ_0

and λ are the emission rate and the emission wavelength, respectively, of an isolated dipole. The radiative line width of the two dipoles is thus given by

$$\Gamma_R(D) = \Gamma_R^0 \cdot (1 + 3\sin(2\pi D/\lambda)/(4\pi D/\lambda)) \qquad (1)$$

where Γ_R^0 is the radiative line width of an isolated dipole.

To compare this distance dependence to the case of the metal nanoparticle pair, we need to extract the radiative line width contribution of the particle pair, Γ_R, from its calculated total line width, Γ. For this purpose, we adopt the approach used in ref 25. Radiative and nonradiative damping processes are assumed to be independent of each other so that $\Gamma_R = \Gamma - \Gamma_{NR}$, where Γ_{NR} is the nonradiative line width contribution of the particle pair. Γ_{NR} is estimated by calculating, in the quasistatic approximation,[1] the line width of a small spheroidal nanoparticle with the same plasmon energy as the particle pair, Γ_{sph}. Because of the use of the quasistatic approximation, Γ_{sph} is purely nonradiative. For a given plasmon energy, the nonradiative damping should depend only on material properties and not explicitly on the particle size nor shape. We may therefore assume $\Gamma_{NR} = \Gamma_{sph}$, and hence $\Gamma_R = \Gamma - \Gamma_{sph}$. The radiative line width contribution determined in this way is plotted in Figure 2a for the same situation as in Figure 1a (black solid line). The dashed horizontal line shows Γ_R for an isolated nanoparticle.

To compare the case of the dipole pair with that of the nanoparticle pair, eq 1 is fitted to the black solid line using λ as a fit parameter. Best agreement is found for $\lambda = 405$ nm (blue line in Figure 2a). In particular, the phase of the oscillations of the particle-pair line width is reproduced well by the fit. The spatial period of the fit, $\lambda = 405$ nm, is close to the emission wavelength of an isolated 80 nm sphere (387 nm in a medium with $n = 1.51$). These agreements lend strong support to the notion that the oscillations of the particle-pair line width are indeed caused by an alternation between constructive and destructive interference of the fields emitted by the two particles. However, we note that the modulation depth of the line width oscillations in the particle case is larger than expected from the point-dipole model. This is the case for all particle sizes studied in our calculations. When the particle diameter is varied from 40 to 100 nm, the initial modulation depth rises from approximately 30% to 50% of the radiative line width of the individual particle. The deviation of the modulation depth is presumably related to the finite diameter of the metal nanoparticles, which is not captured in the point-dipole model.

The black solid line in Figure 2b shows the radiative line width of the nanoparticle pair for longitudinal polarization. For this polarization direction, the radiative line width of two identical point dipoles is given by[40]

$$\Gamma(D) = \Gamma_R^0 \cdot \left(1 - \frac{3\cos(2\pi D/\lambda)}{(2\pi D/\lambda)^2}\right) \qquad (2)$$

The line width calculated according to eq 2 is shown as a blue line in Figure 2b for the same parameter $\lambda = 405$ nm as for the transverse polarization case in Figure 2a. Again, the phase of the oscillations of the particle-pair line width is reproduced well by the point-dipole calculation. The line narrowing of the particle pair at the smallest spacings is a near-field effect that is not included in the point-dipole model and will be discussed later. Compared to the transverse polarization direction, the modulation depth drops off more rapidly with increased spacing D. This is described by the additional $1/D$ dependence of the modulation depth in eq 2 as compared to eq 1. The more rapid drop-off can be explained with the spatial characteristics of the dipole radiation; the fields emitted by each dipole decrease more rapidly with distance along the dipole axis than perpendicularly to it. For longitudinal polarization, this results in a reduced interference along the pair axis and thus a reduced modulation depth of the radiative line width.

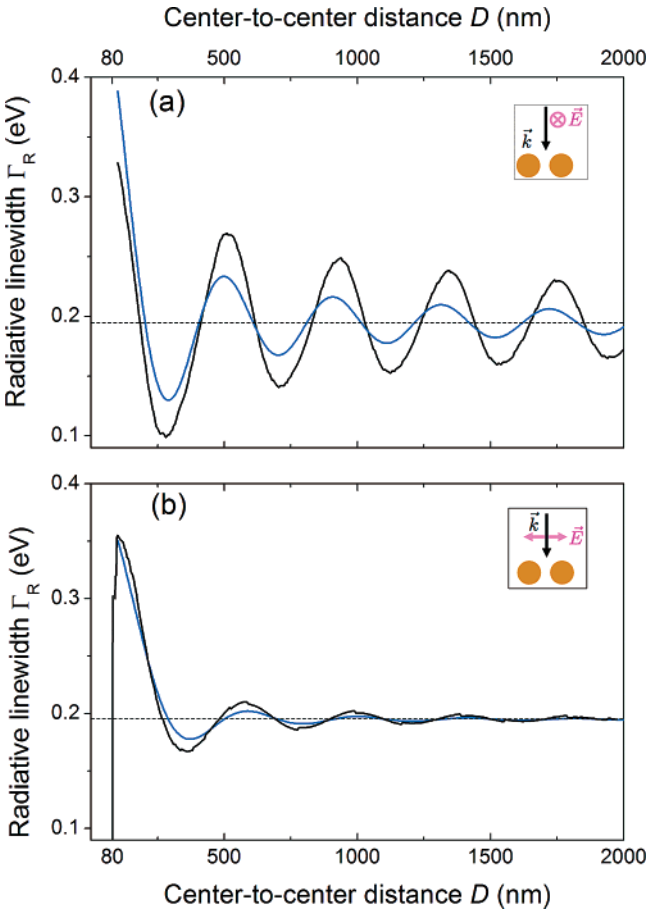

Figure 2. Comparison of the interparticle-distance-dependent radiative line width determined for the nanoparticle pairs of Figure 1 (black solid lines) with calculations for a dipole pair (blue solid lines).[39,40] Figure 2a is for transverse polarization and Figure 2b is for longitudinal polarization. In both figures, the horizontal dashed lines show the radiative line width of an isolated 80 nm gold sphere.

Besides the oscillations in line width, Figure 1 also shows modulations of the plasmon energy, E_p. These modulations may be understood as follows: For certain particle spacings, the electric field emitted by one particle is, at the position of the other particle, parallel to the Coulomb field of the separated charges within that second particle. For those

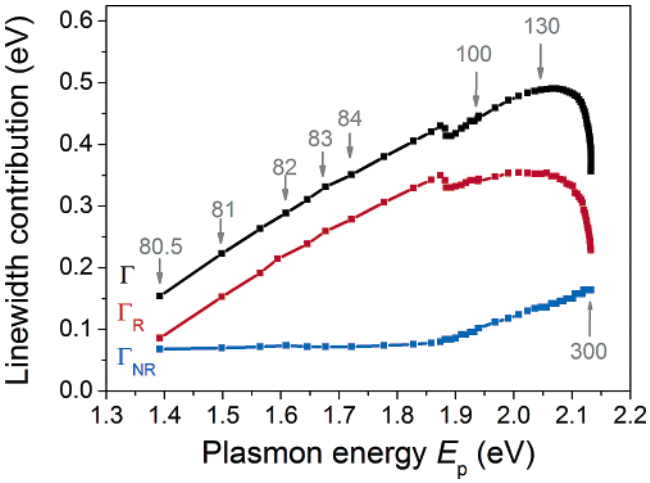

Figure 3. Plasmon line width vs plasmon energy in particle pairs with interparticle (center-to-center) distances $D = 80.5-300$ nm for longitudinal polarization. Some selected values of D (in nm) are indicated by arrows. The total plasmon line width Γ (black curve) is extracted from calculated light-scattering spectra. The contributions of radiative damping Γ_R (red curve) and nonradiative damping Γ_{NR} (blue curve) are obtained as described in the text. The kinks visible at a plasmon energy of ≈ 1.85 eV are artefacts resulting from employing an experimentally obtained dielectric function.[37]

spacings, the total internal field in the second particle and thus the restoring force of the charge oscillation is enhanced, resulting in a blue-shift of the plasmon resonance. Conversely, particle spacings for which the fields are antiparallel result in a red-shift. We note that a similar modification of the restoring force has been suggested to explain the plasmon energy shifts observed in closely spaced nanoparticles, where retardation plays a minor role.[5] In the situation studied here, the modulations of the plasmon energy reaffirm the coupling of the nanoparticles via the emitted far fields, which also was the cause of the modulations in radiative line width. Figure 1 shows that there is a shift between the modulations in plasmon energy and those in line width; this shift is due to the fact that the spacings for which the retarded electric field from one particle is parallel (or antiparallel) to the Coulomb field in the other particle are different from those for which there is maximum interference between the emitted fields from both particles.

Having studied the oscillations in line width and plasmon energy, we will now discuss the line width in the regime of small particle spacings. In this regime, near-field coupling between metal nanoparticles is known to lead to strong red-shifts of the plasmon resonance for longitudinal polarization.[3,7,11,16,17] Such a red-shift is observable for $D < 300$ nm in Figure 1b. For $D < 150$ nm, the red-shift is accompanied by a decrease in plasmon line width to values far below the line width of the isolated plasmon. In the following, we will show that this line narrowing is due to a reduction in radiation damping caused by the plasmonic red-shift.

To illustrate the relation between line narrowing and red shift, the plasmon line width, Γ, is plotted in Figure 3 against the plasmon energy for particle pairs with center-to-center distances $D = 80.5-300$ nm. Also shown are the nonradiative and radiative contributions to the line width, $\Gamma_{NR} = \Gamma_{sph}$ and $\Gamma_R = \Gamma - \Gamma_{sph}$. When reducing the particle spacing from 300 to 130 nm, the plasmon resonance shifts slightly to lower energies, while Γ increases considerably. This line broadening is entirely caused by an increase of Γ_R due to the superradiant effect discussed in the context of Figure 2. In the same range of spacings, Γ_{NR} decreases due to the decreasing importance of interband transitions in gold. The strong line narrowing for spacings $D < 130$ nm cannot be caused by subradiance because the interference between the emitted fields of the two particles is constructive at very small D.

Instead, it may be understood from the frequency dependence of the power radiated by a classical dipole oscillator. If $x(t) = x_0 \cos(\omega t)$ is the separation of the oscillating charges of the dipole, $\pm Q$, their acceleration (which generates the radiation) is given by $\ddot{x}(t) = -x_0\omega_0^2 \cos(\omega_0 t)$. According to elementary electrodynamics, the total (time-averaged) power emitted by the dipole is $\langle dW/dt\rangle \propto \langle (Q\ddot{x})^2\rangle$, and thus $\langle dW/dt\rangle \propto Q^2 x_0^2 \omega_0^4/2$. The total energy of the harmonic oscillator is $W = M\omega_0^2 x_0^2/2$, where M is the mass of the oscillator. This results in a radiative line width

$$\Gamma_R = -\hbar \frac{\langle dW/dt\rangle}{W} \propto \frac{Q^2\omega_0^2}{M} \tag{3}$$

In the case of a particle plasmon, Q and M represent the total charge and mass of all conduction electrons of the particle, respectively, and ω_0 stands for the particle−plasmon frequency. We finally obtain

$$\Gamma_R \propto \hbar\epsilon_0 V \omega_{pl}^2 \omega_0^2 \tag{4}$$

where ϵ_0 is the vacuum permittivity, V is the particle volume, and ω_{pl} is the volume−plasmon frequency, which is connected to the free-electron density n and effective mass m^* via $\omega_{pl} = (ne^2/(\epsilon_0 m^*))^{1/2}$. Our simple treatment thus predicts that the radiative line width of the particle−plasmon resonance should decrease quadratically with particle−plasmon resonance frequency ω_0 due to the slower acceleration of the oscillating electrons at lower frequencies. We note that strong dependencies of the radiation damping on resonance frequency (or wavenumber k) have also been predicted in refs 30, 33, 41, 42. All of this suggests that the line narrowing observed in Figure 3 is a consequence of the plasmon red-shift caused by the reduced particle spacings.

We note that, for the smallest particle spacing regarded here (center-to-center distance $D = 80.5$ nm), Γ_R is reduced by more than 50% with respect to $\Gamma_R = 0.20$ eV for an isolated particle. The plasmon line narrowing caused by the reduced radiation damping implies a reduced dephasing of the coupled plasmon mode, which should lead to a larger local-field enhancement in the interstitial region between the particles.[7,10,11]

In summary, radiation damping in pairs of metal nanoparticles, which may serve as a model system for more complex nanoparticle systems, was studied theoretically. The

radiation damping rate of plasmons in pairs of spherical gold nanoparticles was extracted from light-scattering spectra calculated using generalized Mie theory. In these calculations, retardation effects are taken into full account. Far-field coupling between the nanoparticles over distances many times the particle diameter was found. The radiation damping of the coupled particle−plasmon mode alternates between superradiative and subradiative behavior when the partice spacing is varied. The large modulations of the line width observed here imply that care must be taken when electromagnetic coupling between relatively widely spaced particles is assumed to be negligible, as is often done in experiments on nanoparticles ensembles. At small particle spacings where near-field coupling occurs, the radiation damping rate lies far below that of an isolated particle. This reduction of radiation damping implies a reduced dephasing of the coupled plasmon mode and thus tends to increase the local field enhancement in the space between the particles. This effect should be beneficial for nonlinear optical applications such as surface-enhanced Raman spectroscopy.[10,20,23]

We thank A. Christ, J. Feldmann, T. Franzl, H. Giessen, T. Klar, S. Kowarik, H.-J. Kull, M. Reismann, and C. Sönnichsen for discussions and A. Sprafke for assistance in preparing some figures of the manuscript. Financial support by the DFG through project no. PL 261/4−1 and Graduiertenkolleg 1035 is acknowledged.

References

(1) Kreibig, U.; Vollmer, M. *Optical Properties of Metal Clusters*, 25th ed.; Springer Series in Materials Science; Springer: Berlin, 1995.
(2) Link, S.; El-Sayed, M. A. *J. Phys. Chem. B* **1999**, *103*, 8410−8426.
(3) Aravind, P. K.; Nitzan, A.; Metiu, H. *Surf. Sci.* **1981**, *110*, 189−204.
(4) Tsai, D. P.; Kovacs, J.; Wang, Z.; Moskovits, M.; Shalaev, V. M.; Suh, J. S.; Botet, R. *Phys. Rev. Lett.* **1994**, *72*, 4149−4152.
(5) Rechberger, W.; Hohenau, A.; Leitner, A.; Krenn, J.; Lamprecht, B.; Aussenegg, F. *Opt. Commun.* **2003**, *220*, 137−141.
(6) Fromm, D. P.; Sundaramurthy, A.; Schuck, P. J.; Kino, G.; Moerner, W. E. *Nano Lett.* **2004**, *4*, 957−961.
(7) Hao, E.; Schatz, G. *J. Chem. Phys.* **2004**, *120*, 357−366.
(8) Nordlander, P.; Oubre, C.; Prodan, E.; Li, K.; Stockman, M. I. *Nano Lett.* **2004**, *4*, 899−903.
(9) Kottmann, J.; Martin, O. J. F. *Opt. Exp.* **2001**, *8*, 655−663.
(10) Kottmann, J.; Martin, O. J. F. *Opt. Lett.* **2001**, *26*, 1096−10098.
(11) Xu, H.; Aizpurua, J.; Käll, M.; Apell, P. *Phys. Rev. E* **2000**, *62*, 4318−4324.
(12) Maier, S. A.; Brongersma, M. L.; Kik, P. G.; Atwater, H. A. *Phys. Rev. B* **2002**, *65*, 193408.
(13) Li, K.; Stockman, M. I.; Bergman, D. J. *Phys. Rev. Lett.* **2003**, *91*, 227402.
(14) Zou, S.; Janel, N.; Schatz, G. *J. Chem. Phys.* **2004**, *120*, 10871−10875.
(15) Muhlschlegel, P.; Eisler, H.-J.; Martin, O. J. F.; Hecht, B.; Pohl, D. W. *Science* **2005**, *308*, 1607−1609.
(16) Schmeits, M.; Dambly, L. *Phys. Rev. B* **1991**, *44*, 12706−12712.
(17) Pack, A.; Hietschold, M.; Wannemacher, R. *Opt. Commun.* **2001**, *194*, 277−287.
(18) Sönnichsen, C.; Reinhard, B. M.; Liphard, J.; Alivisatos, A. P. *Nat. Biotechnol.* **2005**, *23*, 741−745.
(19) Krenn, J. R.; Dereux, A.; Weeber, J. C.; Bourillot, E.; Lacroute, Y.; Goudonnet, J. P.; Schider, G.; Gotschy, W.; Leitner, A.; Aussenegg, F. R.; Girard, C. *Phys. Rev. Lett.* **1999**, *82*, 2590−2593.
(20) Jiang, J.; Bosnick, K.; Maillard, M.; Brus, L. *J. Phys. Chem. B* **2003**, *107*, 9964−9972.
(21) Podolskiy, V. A.; Sarychev, A. K.; Shalaev, V. M. *J. Nonlinear Opt. Phys. Mater.* **2002**, *11*, 65−74.
(22) Grigorenko, A. N.; Geim, A. K.; Gleeson, H. F.; Zhang, Y.; Firsov, A. A.; Khrushchev, I. Y.; Petrovic, J. *Nature* **2005**, *438*, 335−338.
(23) Wokaun, A.; Gordon, J.; Liao, P. *Phys. Rev. Lett.* **1982**, *48*, 957−960.
(24) Klar, T.; Perner, M.; Grosse, S.; von Plessen, G.; Spirkl, W.; Feldmann, J. *Phys. Rev. Lett.* **1998**, *80*, 4249−4252.
(25) Sönnichsen, C.; Franzl, T.; Wilk, T.; von Plessen, G.; Feldmann, J.; Wilson, O.; Mulvaney, P. *Phys. Rev. Lett.* **2002**, *88*, 77402.
(26) Hövel, H.; Hilger, A.; Kreibig, U.; Vollmer, M. *Phys. Rev. B* **1993**, *48*, 18178−18188.
(27) Stietz, F.; Bosbach, J.; Wenzel, T.; Vartanyan, T.; Goldmann, A.; Träger, F. *Phys. Rev. Lett.* **2000**, *84*, 5644−5647.
(28) Berciaud, S.; Cognet, L.; Tamarat, P.; Lounis, B. *Nano Lett.* **2005**, *5*, 515−518.
(29) Novo, C.; Gomez, D.; Perez-Juste, J.; Zhang, Z.; Petrova, H.; Reismann, M.; Mulvaney, P.; Hartland, G. V. *Phys. Chem. Chem. Phys.* **2006**, *8*, 3540−3546.
(30) Persson, B. N. J.; Baratoff, A. *Phys. Rev. Lett.* **1992**, *68*, 3224−3227.
(31) Scharte, M.; Porath, R.; Ohms, T.; Aeschlimann, M.; Krenn, J. R.; Ditlbacher, H.; Aussenegg, F. R.; Liebsch, A. *Appl. Phys. B* **2001**, *73*, 305−310.
(32) Buchler, B. C.; Kalkbrenner, T.; Hettich, C.; Sandoghdar, V. *Phys. Rev. Lett.* **2005**, *95*, 063003.
(33) Melikyan, A.; Minassian, H. *Appl. Phys. B* **2004**, *78*, 453−455.
(34) Lamprecht, B.; Schider, G.; Lechner, R. T.; Ditlbacher, H.; Krenn, J. R.; Leitner, A.; Aussenegg, F. R. *Phys. Rev. Lett.* **2000**, *84*, 4721−4724.
(35) Gérardy, J.; Ausloos, M. *Phys. Rev. B* **1982**, *25*, 4204−4229.
(36) Quinten, M.; Kreibig, U. *Appl. Opt.* **1993**, *32*, 6173−6182.
(37) Johnson, P. B.; Christy, R. W. *Phys. Rev. B* **1972**, *6*, 4370−4379.
(38) Additional calculations (not shown here) demonstrate that the agreement between the period of the oscillations and the plasmon peak wavelength also holds in media with refractive indices different from 1.51.
(39) DeVoe, R. G.; Brewer, R. *Phys. Rev. Lett.* **1996**, *76*, 2049.
(40) Coherent interaction of two trapped ions by R. G. DeVoe. In *Quantum Dynamics of Simple Systems; The Forty-Fourth Scottish Universities Summer School in Physics, Stirling, August 1994*; Oppo, G. L., Barnett, S. M., Riis, E., Wilkinson, M., Eds.; Institute of Physics Publishing: Bristol, UK, 1996.
(41) Gersten, J. I.; Nitzan, A. *J. Chem. Phys.* **1981**, *75*, 1139−1152.
(42) Meier, M.; Wokaun, A. *Opt. Lett.* **1983**, *8*, 581−583.

NL062377U